Original study on mathematical models for analysis of cellulose water content from absorbance/wavenumber shifts in ATR FT-IR spectrum

Stefan Cichosz
Lodz University of Technology
Anna Masek (anna.masek@p.lodz.pl)
Lodz University of Technology
Katarzyna Dems-Rudnicka
Lodz University of Technology

Research Article

Keywords: cellulose, moisture content, Fourier-transform infrared spectroscopy, linear models

Posted Date: July 21st, 2022

DOI: https://doi.org/10.21203/rs.3.rs-1860641/v1

Abstract

The aim of this research was to evaluate the applicability of the attenuated total reflectance Fourier-transform infrared (ATR FT-IR) spectroscopy in the quantitative analysis of the moisture content in cellulose (from 0.5-11.0wt.%). Innovatively, this work describes for the first time the variations in both absorbance and wavenumber of 16 absorption bands plotted as a function of cellulose water amount measured with Karl-Fischer titration. Different regression models were investigated (simple linear, semilogarithmic, power) and the adjusted coefficient of determination (R^2) was given for each calculation. While model exhibited R^2>90%, the standard error of calibration (SEC) was presented and an external validation has been performed. Regarding the absorbance-water content relationship, data recorded for sixteen peaks was successfully fitted with linear functions exhibiting R^2>90%. The highest value of R^2=98.7% and standard error of prediction SEP=6.0% have been assigned to the maximum from 3339-3327 cm^{-1} (-OH), proving ATR FT-IR usefulness in quantitative analysis.

1. Introduction

Most commonly, time- and money-consuming techniques are employed for the determination of moisture content in natural fibres, e.g., thermogravimetric analysis (TGA) (Gašparovič et al. 2010; Cheng and Heidari 2017) or Karl-Fischer titration (Martin et al. 2013; Przybylek 2017). Yet, in the recent years, attenuated total reflectance Fourier-transform infrared (ATR FT-IR) spectroscopy has been repeatedly proposed as a fast, cost-effective and non-invasive method in monitoring the moisture absorption processes in polymer-based systems (Célino et al. 2014; Hou et al. 2014; Yuan et al. 2019; Consumi et al. 2021). Undoubtedly, this technique provides many attractive features, e.g., high sampling rate, sensitivity and the information at the molecular level contained in the vibrational spectra (Hospodarova et al. 2018; Käppler et al. 2018). Importantly, the development of attenuated total reflectance (ATR) FT-IR spectroscopy techniques enabled the use of this method directly onto solid materials (Hou et al. 2014; Canteri et al. 2019). Thus, making it easy to use in both industrial and scientific facilities. Below, some examples of the studies considering employment of ATR FT-IR spectroscopy technique in moisture content determination of cellulose-based materials have been discussed.

Firstly, Hou et al. (Hou et al. 2014) have investigated the kinetics of water diffusion through the ethyl cellulose (EC) films plasticized with triethyl citrate (TEC). The films analysed were casted from 2wt.% alcoholic solutions of EC/TEC, dried and then subjected to the water absorption. The spectral data has been collected as a function of time with acquisition interval of 40 s. Importantly, the analysed data was collected only during a single experiment, hence, it did not provided information on the reproducibility of investigated processes. The normalized ATR FT-IR spectra of dried EC-based films containing from 0-30wt.% TEC were investigated. The authors focused mainly on the region 3700-3100 cm^{-1} that is closely related to the O-H stretching vibration of water molecules (Oh et al. 2005a). It has been observed that the intensity of the O-H stretching band was gradually increasing in the first 2 h for all the investigated diffusion systems. Then, the researchers calculated the integrated areas of the O-H stretching region and

plotted it as a function of diffusion time to obtain moisture diffusion curves. Moreover, to identify the functional groups participating in the water diffusion process, all the ATR FT-IR spectra at equal time intervals of 40 s were selected to carry out 2Dcos analysis. However, the 2D asynchronous maps were drawn only for the region 3700-3100 cm^{-1}, thus revealing the spectral changes in a narrow sector of IR spectrum corresponding to the vibrations of hydroxyl moieties.

Similarly, Consumi et al. (Consumi et al. 2021) have come to the congruous conclusions. However, the authors used k-fold cross-validation technique based on the enlarged dataset of 80 samples divided into k = 5 folds. The researchers investigated carboxymethyl cellulose (CMC) of a varied moisture content and found that the intensities of the bands related to the stretching vibration of OH group (broad absorption band at 3392 cm^{-1} and a shoulder at 3255 cm^{-1}) were significantly affected by the moisture presence. The authors determined the total area under the ATR FT-IR curve in the range 3675-2980 cm^{-1} and plotted it against the moisture content in cellulose sample. A simple linear regression including all the experimental data and IR band areas showed a good fit. Moreover,
a satisfying correlation between the measured and predicted data was found for all the five training sets.

However, Célino et al. (Célino et al. 2014) have concluded that not only a broad peak from 3700-3000 cm^{-1} might be useful in the quantitative analysis of water content in cellulose-based systems. *The authors investigated the spectral signatures of various raw plant fibres, namely, hemp, flax and sisal at different moisture contents. The researchers described the molecular effect of water sorption mechanisms and employed a multivariate model linking different regions of FT-IR spectra. The model was developed using partial least square regression (PLS-R) and the data has been gathered from single water absorption experiment at a certain relative humidity. Firstly, the researchers performed Kruskal Wallis analysis on each individual wavenumber of the raw spectra. It highlighted several zones of the FT-IR fingerprint that were strongly impacted by the increasing water uptake: i. the broad band situated between 3600-3000 cm^{-1}; ii. the maximum at 1635 cm^{-1}; iii. the band placed in the wavenumber ranging from 1100-700 cm^{-1}. Surprisingly, according to the Kruskal Wallis p-values assignment conducted by the researchers, the CH stretching band situated at 2935-2900 cm^{-1} was also found to be significantly impacted by the water uptake. Finally, the models were calculated promptly from the information contained in the spectral regions situated from 3600-3000 cm^{-1} and around 1650 cm^{-1}. According to the authors, these maxima were associated to the main regions characteristic of the water-biopolymer interactions, while the remaining absorption bands have been excluded and assigned to the materials' intrinsic variability.*

Furthermore, Yuan et al. (Yuan et al. 2019) also tried to determine different IR regions useful in the quantitative analysis of the water content in cellulose-based systems. Nevertheless, the authors of this work have employed a slightly different approach. The researchers presented an interesting study on the moisture content determination in TEMPO oxidized cellulose nanocrystal film (TOCNF). Water content of TOCNF was collected using the dynamic vapor sorption (DVS) apparatus. Then, the results were correlated with recorded ATR FT-IR spectra. The researchers noted that the main band at 3347 cm^{-1}, assigned to the OH group, has changed significantly during the moisture absorption process. Meanwhile,

the weaker maximum located next to 1608 cm^{-1} and attributed to C-O-C asymmetric stretching vibration was observed to shift toward lower wavenumbers. Moreover, the authors also pointed out that with an increasing relative humidity the intensity of the band at 1171 cm^{-1} has been gradually falling while the absorbance of the peak situated at 1159 cm^{-1} was rising. Based on this, the researchers concluded that primarily three spectrum ranges correlate with the moisture adsorption in cellulose-based materials: 3700-3000 cm^{-1}, 1700-1580 cm^{-1} and 1180-1140 cm^{-1}. The authors also employed PLS-R method during the data analysis.

Contrary to the researches discussed above, this study relies on the data collected from 25-times-repeated moisture absorption/desorption experiments, hence, including the aspect of reproducibility, and employs a dedicated protocol of a mathematical analysis created for the purposes of the submitted research. Therefore, this research presents for the first time a reliable statistic-based peak-by-peak investigation of both the absorbance and wavenumber shifts of 16 absorption bands visible in cellulose IR spectrum plotted as a function of moisture amount established with Karl-Fischer titration. Moreover, instead of commonly used PLS-R technique, three regression models were investigated: simple linear, semilogarithmic, power. When the adjustment exhibited R^2 > 90%, an external validation has been performed with ten additional IR-Fischer titration data packages. Consequently, the approach presented is a scientific novelty and the most cautious analysis done. Accordingly, this work undoubtedly provides the knowledge broadening on the IR spectrum employment possibilities as a non-destructive technique used in quantitative assessment of water content in cellulose.

2. Materials And Methods

2.1. Materials

Cellulose fibres of a length between 6–12 μm, trade name Arbocel UFC100 Ultrafine Cellulose for Paper and Board Coating, with a density referred as 1.3 g/cm^3 and pH range from 5.0-7.5 was delivered by J. Rettenmaier & Söhne (Rosenberg, Germany). Moreover, phosphorus oxide (V) and potassium nitrate were purchased from Chempur (Poland, Piekary Slaskie) and employed as the desiccator cartridges for, respectively, cellulose conditioning and moisture absorption experiment. Phosphorous oxide (V) is a solid that exhibits pH of approximately 1.5 and density of about 2.3 g/cm^3. It is referred to provide an atmosphere of the relative humidity (RH) of approximately 0% (Mihranyan et al. 2004b). In turn, the solubility of potassium nitrate in water is on the level of 316 g/L (20°C). According to literature, its saturated aqueous solution is able to provide the atmosphere of a specific relative humidity which is approximately 96% (Mihranyan et al. 2004b). Additionally, Hydranal Solvent E and Hydranal Titrant 5E, used during Karl-Fischer titration experiment, were supplied by Honeywell Fluka (Loughborough, UK).

2.2. Methods

2.2.1. Preparation of cellulose specimens of a varied moisture content

Cellulose studied in this research has been divided between separate weighing bottles (35x70 mm) with 0.1 g (Fourier-transform infrared spectroscopy) or 1.5 g (Karl Fischer titration) of cellulose in each vessel. Importantly, a separate weighing bottle for a separate FT-IR/titration experiment has been prepared. Next, cellulose conditioning, moisture absorption and desorption experiments were caried out: i. cellulose conditioning in the desiccator filled with phosphorus oxide (RH = 0%) for 7 days (all prepared weighing bottles with cellulose); ii. moisture absorption experiment: desiccator filled with saturated solution of potassium nitrate; experiment lasted 24 h, measurements after 0, 1, 3, 5, 8, 24 h (the last measurement after 24 h is the beginning of the moisture desorption stage at 0 h); iii. moisture desorption experiment: laboratory dryer (Binder, Tuttlingen, Germany) at 100°C for 8 h, measurements after 0, 1, 3, 5, 8 h. To obtain reliable results, the described above process of moisture absorption/desorption by cellulose was repeated 25 times. Then, the amount of n = 250 spectra were recorded.

2.2.2. Determination of cellulose properties

2.2.2.1. Fourier-transform infrared spectroscopy

Fourier transform infrared spectroscopy (FT-IR) absorbance spectra were recorded within

the 4000 – 400 cm^{-1} range. To ensure an acceptable signal-to-noise ratio, 64 scans at resolution of 4 cm^{-1} were accumulated (absorption mode). The experiment has been performed with the use of Thermo Scientific Nicolet 6700 FT-IR spectrometer equipped with diamond Smart Orbit iTX attenuated total reflection (ATR) sampling accessory (Waltham, MA, USA). Recorded spectra were baseline corrected with OMNIC 9.2.86 software.

2.2.2.2. Karl-Fischer titration

At the same time as FT-IR experiment, Karl-Fischer titration was carried out with the use of TitroLine Alpha (Schott, Mainz, Germany) device. For each experiment approximately 1.3 g of cellulose sample and 30 ml of Hydranal Solvent E were taken.

2.2.2.3. Data analysis

Coordinates (absorbance, wavenumber) of the selected peaks from IR spectra were read and plotted as a function of moisture content in cellulose fibres determined with Karl-Fischer titration. Then, RStudio (version 1.4.1106) software was employed in data analysis (R Core Team 2021). Tree models, namely, simple linear (Eq. 3), semilogarithmic (Eq. 4), power (Eq. 5), were investigated to find the relationship between variables:

$$Y = a \bullet X + b (3)$$

$$Y = a \bullet \ln(X) + b (4)$$

$$Y = a_1 X^{b_1} \Longleftrightarrow \ln(Y) = a \bullet \ln(X) + b (5)$$

Y refers to a measured parameter (absorbance or wavenumber) read from IR spectrum and X is a moisture content. First, the simple linear model was assessed. If the analysed data did not show a linear relationship, two successive models (semilogarithmic, power) were examined. The quality of the models was estimated using the adjusted coefficient of determination (R^2) and standard error value for calibration (SEC). Additionally, an independent data set used for the model external validation (10 samples of recorded IR spectrum and determined moisture content) has been employed to assess prediction adequacy with adjusted coefficient of determination and standard error for prediction (SEP). For a reliable model, the R^2 values should be high, while SEC and SEP values should be as low as possible. Graphs were prepared using *ggplot2* package from the program mentioned above.

3. Results And Discussion

3.1. Linear models assessed

In this study, the variations of X- and Y-axis coordinates of sixteen selected peaks were investigated and plotted as a function of moisture content. This means, not the changes in the spectrum heigh at the specified and fixed positions were measured, but the cautious evaluation on the real maxima coordinates of sixteen selected peaks has been conducted. Therefore, the approach presented relevantly differs from previously performed studies (Célino et al. 2014; Hou et al. 2014; Yuan et al. 2019; Consumi et al. 2021). It accounts the movements of the absorption bands' maxima along both the axes of frequency and absorbance, as well as considers sixteen different peaks attributed to chemical groups embodied in cellulose structure. Consequently, revealing what happens with a peak's highest point while cellulose moisture content elevates. Tracking the changes at a fixed wavelength might be misleading as it does not reflect a full spectral information on the chemical groups embodied in cellulose and their interactions with water molecules, e.g., possible shifts of some absorption bands along the frequency axis. Moreover, a not assigned random wavelength is a parameter without any significant scientific information – it is just a mathematical coordinate.

Absorption bands taken into consideration in this study are presented in **Fig. 1**. Sixteen selected maxima have been marked with red dots. Each red dot represents a point regarded for further mathematical analysis and the dashed lines reveal how the coordinates (X – wavenumber, Y – absorbance) have been read. The total amount of investigated cellulose samples is n = 250.

Moreover, **Table 1** gathers information about a chemical meaning behind the selected absorption bands and reveals the assignment of sixteen maxima to the chemical moieties present in the structure of investigated biopolymer. Further information on the interpretation of cellulose IR spectrum is available elsewhere (Oh et al. 2005a; Cichosz and Masek 2020). Noteworthily, the wavenumber range given in **Table 1** shows the variations between the lowest and the highest wavenumber values attributed to the position of the absorption band's maximum in the recorded IR spectra.

Table 1 Assignment of the analysed absorption bands to chemical moieties embodied in cellulose structure.

Peak no.	*Wavenumber range [cm^{-1}]*	*Chemical group*	*Ref.*
1.	444-432	vibration of C-O bonds	(Kaur et al. 2012)
2.	560-556	γCH, characteristic of cellulose I	(Chen et al. 2020)
3.	668-660	δCOH out of plane	(Lee et al. 2015)
4.	900-895	γCOC at β-glycosidic linkage; amorphous region	(Oh et al. 2005b)
5.	1032-1027	γCO	(Lee et al. 2015)
6.	1056-1051	γCO	(Lee et al. 2015)
7.	1107-1103	γ ring in plane	(Gulmine et al. 2002)
8.	1162-1159	γCOC at β-glycosidic linkage	(Oh et al. 2005b)
9.	1203-1199	δCOH in plane	(Oh et al. 2005b)
10.	1316-1314	δCH_2 (wagging)	(Poletto et al. 2014)
11.	1335-1332	δCOH in plane	(Olsson and Salmén 2004)
12.	1370-1360	δCH	(Ciolacu et al. 2011)
13.	1429-1425	δCH_2 (symmetric); crystalline region	(Oh et al. 2005b)
14.	1646-1636	absorbed water	(Oh et al. 2005b)
15.	2898-2888	γCH	(Morán et al. 2008)
16.	3339-3327	γOH covalent bond, hydrogen bonding	(Oh et al. 2005a)

Furtherly, as every cellulose IR analysis performed was accompanied by a short and precise Karl-Fischer titration experiment, the moisture content of each biopolymer sample has been successfully established. Then, the coordinates of absorption bands' maxima, namely, both absorbance and wavenumber, were plotted as a function of water content in cellulose specimens. Consequently, to reduce the studied dependencies to a linear form, the regression adjustment has been performed separately for each peak. The results of the carried out investigation for three different models (simple linear, semilogarithmic, power) have been gathered in **Table 2**. The adjusted coefficient of determination (R^2) was given for each model analysed. Furthermore, in case of absorbance-based models that exhibited $R^2 > 90\%$ the standard error of calibration (SEC) was presented as well. Importantly, an external validation has been performed with ten additional IR-Fischer titration data packages.

From the information presented in **Table 2**, it is clearly visible that ATR FT-IR technique has a great potential as a tool in quantitative determination of water content in cellulose. It might be concluded that the absorbance-based simple linear model favourably described the gathered data, because R^2 assigned to the simple linear fits for all peaks investigated exhibited a value higher than 90%. Therefore, the remaining semilogarithmic and power models have not been taken into consideration. Yet, regarding the wavenumber-based models, all three fits were investigated and none of them exhibited a value of R^2 higher than 90%, hence, they did not describe the data with a sufficient reliability. Among the analysed models, the highest coefficients of determination values were at the level of approximately 70-75%.

Further description of the models analysed in this study, as well as the observed changes of the peaks' coordinates with raising moisture content of cellulose have been presented in the subsequent sections of the article.

Table 2 Quality parameters for models' calibration and external set validation for the models selected (p-value for each regression on the level <0.5); SEC – standard error of calibration, SEP – standard error of prediction, R^2 – adjusted coefficient of determination.

Peak no.	*Absorbance-based simple linear model*				*Wavenumber-based calibration*		
	Calibration		*External validation*				
	SEC [%]	*R^2 [%]*	*SEP [%]*	*R^2 [%]*	*Simple linear model R^2 [%]*	*Semilogarithmic model R^2 [%]*	*Power model R^2 [%]*
1.	0.9	96.9	11.9	99.2	10.6	10.2	10.2
2.	0.8	96.3	12.7	99.1	70.0	75.6	75.6
3.	7.5	96.8	12.7	99.1	65.7	64.9	64.9
4.	8.3	95.9	9.7	99.5	13.4	9.8	9.8
5.	8.8	92.0	14.6	98.8	41.4	46.4	46.4
6.	7.9	92.8	14.4	98.9	64.0	69.0	69.0
7.	7.0	94.0	13.0	99.1	9.6	16.4	16.4
8.	6.4	95.6	11.2	99.3	30.1	50.3	50.3
9.	9.7	93.1	11.2	99.3	66.4	66.7	66.7
10.	6.6	97.0	9.4	99.5	4.8	3.7	3.7
11.	6.8	96.5	9.2	99.5	45.4	51.2	51.2
12.	7.0	96.4	9.5	99.5	41.8	48.6	48.5
13.	7.5	96.3	10.0	99.5	46.4	50.5	50.5
14.	22.5	92.6	18.3	98.3	2.3	1.8	1.8
15.	8.9	94.9	12.2	99.2	58.3	49.0	49.0
16.	5.7	98.7	6.0	99.8	6.1	8.0	8.0

3.2. Absorbance-moisture content dependency

Fig. 2 reveals the experimental data regarding the changes in the absorbance values (height of the peak) assigned to sixteen maxima visible in IR spectrum of cellulose fibres. Additionally, the black lines represent the regression functions that coefficients of determination (R^2) and standard errors of calibration (SEC) have been shown in **Table 2**.

Giving a closer look at **Fig. 2**, it might be easily perceived that absorbance of each peak analysed is changing significantly while the moisture content in cellulose specimens elevates. The similar phenomenon has been observed by some other scientists (Célino et al. 2014; Hou et al. 2014; Yuan et al. 2019; Consumi et al. 2021). However, in this study the raise in the height of each peak recorded, for the

first time, have been successfully described with linear functions exhibiting R^2 > 90%. High value of adjusted determination coefficient means the models applied reliably reflected the experimental data.

Interestingly, signals originated from both oxygen-embodying (peaks no.: 1, 3, 4, 5, 6, 8, 9, 11, 16) and oxygen-lacking (peaks no.: 2, 7, 10, 12, 13, 15) chemical groups responded to the variations in moisture content in cellulose fibres. It is not surprising that changes in the maxima assigned to oxygen-rich chemical moieties, being able to form hydrogen bonds with water molecules, altered during the water absorption process (Mihranyan et al. 2004a). Due to the differences in the electronegativity between the atoms in oxygen-embodying groups, these moieties are able to create electrostatic attraction between cellulose and water molecules. Consequently, water bonds to the cellulose surface via physical forces (Hofstetter et al. 2006; Salmén and Bergström 2009). Because of the changes in cellulose-water interactions, the investigated chemical groups differently reacted to the infrared radiation and absorbance/wavenumber shifts of the peaks could have become visible in IR spectrum (peaks no.: 1, 3, 4, 5, 6, 8, 9, 11, 16).

However, it is not certain what kind of mechanism stands behind the recorded variations in absorbance/wavenumber of the peaks assigned to non-polar CH_2 and C-H chemical groups that are not able to directly interact with water molecules (peaks no.: 2, 7, 10, 12, 13, 15). Nevertheless, Celino et al. (Célino et al. 2014) proposed a theory that could bring some elements of understanding. The changes observed might be favourably described with the surrounding signals originated from oxygen-embodying chemical moieties. The shoulders of the maxima assigned to carbon- and oxygen-rich chemical groups overlap, hence, affecting the shape, as well as the height of the peaks visible in IR spectrum.

Another explanation has been proposed by Yuan et al. (Yuan et al. 2019) who concluded that IR spectrum might also react to the cellulose chain stiffening caused by moisture absorption. The scientists referred that the changes in the macromolecule's stiffness might contribute to the shifts along both absorbance and frequency axes.

Furtherly, the attention should be drawn to some interesting results that have been shown in **Fig. 2n**. Peak no. 14 is generally assigned to the moisture absorbed in cellulose (water content) (Oh et al. 2005b). Importantly, this maximum is not present in IR spectrum of the biopolymer in a dried state. Therefore, its appearance could be only related to the water absorbed by cellulose fibres. Consequently, it should precisely reflect the amount of moisture bonded to cellulose. However, an opposite effect could have been observed. Peak no. 14 exhibits one of the lowest values of adjusted determination coefficient R^2 = 92.6% and the highest standard error of calibration SEC = 22.5% (**Table 2**). This means, the mathematical function applied does not precisely reflect the experimental data.

This observation could be explained with the nature of a certain peak. Often, maxima visible in IR spectrum are the common effect of many smaller signals that overlap. Therefore, their position and height are determined by many different interactions (Bledzki et al. 2002; Łojewska et al. 2005; Kondo et al. 2016), e.g. hydrogen bonds (Peršin et al. 2011), van der Waals forces (Missoum et al. 2013). However,

peak no. 14 is assigned only to the moisture content in cellulose fibres. Hence, it reflects merely the vibrations of water molecules. Probably, this absorption band might be hardly deconvoluted into separated signals and could be significantly affected by the shoulders of neighbouring maxima. Therefore, the peak's position is not stable and highly influenced by its surrounding.

Taking into account the above reasoning, if assume that peaks consisting of multiple signals and separated from the remaining absorption bands (restricted overlapping with neighbouring maxima) describe water uptake more reliably, a mathematical model assigned to an alone absorption band that might be deconvolved into different signals (especially corresponding to water-cellulose hydrogen bonds) should more accurately describe the changes in cellulose moisture content. Interestingly, this theory has found a confirmation in practice. The highest value of the adjusted coefficient of determination (R^2 = 98.7%) has been recorded for partially separated peak no. 16 that could be successfully deconvoluted into three types of hydrogen bonding: intramolecular (3OH···O5 and 2OH···O6), intermolecular (6OH···O3') (Łojewska et al. 2005; Oh et al. 2005a). Most likely, the position of this peak is stabilized with three species of interactions that might be affected by the presence of water molecules, as moisture bonds to the same active centres that create inter- and intramolecular hydrogen bonds in cellulose structure. Then, the outcome is a describable and observable peak's shift along the Y axis.

Next, all investigated models have been validated with external experimental data set. The results of the validation performed are presented in **Table 2** and **Fig. 3**. The mathematical functions developed in this study revealed the satisfactory similarity between the newly recorded data and the values predicted with the linear functions. The coefficients of determination for validated models exhibited values from 98.3-99.8% with the best fit for peak no. 16, which is also easily visible with a naked eye while comparing the graphs presented in **Fig. 3**. This means, the information collected with ATR FT-IR technique could be successfully correlated with volumetric measurements of moisture content in cellulose (e.g., Karl-Fischer titration). Consequently, ATR FT-IR method might be favourably regarded as a quantitative technique for the determination of moisture content in cellulose fibres.

Yet, the data presented in this study could be investigated differently. Experimental points of each peak characterised (**Fig. 2**) may be favourably divided into two parts depending on a specific bend in the shape created by the plotted data: the first stage from approximately 0-2wt.% of moisture content (before the bend) and the second stage from 2-10wt.% (after the specific bend). Therefore, this alternative approach has been carefully analysed regarding the adjustment of linear models analysed in this study, namely: simple linear fit, semilogarithmic, power. Results of this additional analysis are presented in **Table 3**.

Table 3 Quality parameters of fit adjustment for the alternative two-stage approach of data analysis (in case of most correlations evaluated p-value on the level <0.5); SEC – standard error of calibration, SEP – standard error of prediction, R^2 – adjusted coefficient of determination.

Peak no.	*1st stage (moisture content: 0-2wt.%)*			*2nd stage (moisture content: 2-10wt.%)*
	Simple linear model R^2 [%]	*Semilogarithmic model R^2 [%]*	*Power model R^2 [%]*	*Simple linear model R^2 [%]*
1.	69.9	85.8	83.1	93.2
2.	69.1	86.9	81.5	92.1
3.	67.9	85.7	82.4	93.0
4.	58.0	71.0	69.8	91.6
5.	57.5	72.9	65.6	86.1
6.	56.2	72.0	64.7	88.1
7.	57.5	73.8	68.3	90.4
8.	57.8	74.3	70.2	92.4
9.	34.4	42.9	42.6	88.4
10.	63.9	80.5	77.5	94.1
11.	60.6	76.1	73.7	93.5
12.	60.6	76.4	73.3	93.1
13.	55.1	69.0	67.0	92.8
14.	1.1*	1.6*	1.2*	89.4
15.	65.7	83.2	79.2	89.1
16.	74.9	93.2**	87.4	97.8**

* p-value > 0.5

** Calibration: SEC = 0.001%, External validation: SEP = 6.2%, R^2 = 99.8%

Nonetheless, the division did not result in a more precise description of experimental points. Taking into consideration values of the coefficients of determination (**Table 3**), almost none of the mathematical models was able to reliably describe the changes in experimental points at the 1st stage of moisture absorption (moisture content: 0-2wt.%). However, simple linear fit, again, successfully reflected the increase in absorbance with raising water content during the 2nd stage of moisture absorption process (moisture content: 2-10wt.%).

Similarly, as in the previous investigation, the most adequate adjustment has been observed for the peak no. 16 which underlines the reliability of this absorption band regarding the possibility of quantitative analysis of water content in cellulose-based systems. The 1st stage of moisture absorption could have been efficiently described with semilogarithmic model (R^2 = 93.2%, SEC = 0.001%) and the 2nd stage – with simple linear fit (R^2 = 97.8%, SEP = 6.2%).

Taking into account the considerations set out above, it would be also worth considering whether it is reasonable to use only one absorption band to determine the water content of natural cellulose fibres, or whether the results calculated from the different absorption bands should be averaged. Therefore, additional calculations were made. The determined moisture contents obtained from the 16 absorption bands were averaged for each experimental point. Then, external validation was performed. The adjusted coefficient of determination was at the level of R^2 = 99.5%, and the standard SEP prediction error – SEP = 9.9%. These values indicate a slightly lower accuracy of such a method along with the determination of the moisture content in cellulose for, e.g., peak no. 16. Thus, proving once again the accuracy of the determinations made using this absorption band.

3.3. Wavenumber-moisture content relationship

Additionally, this is the first study that have deeply investigated the wavenumber-moisture content relationship and the possibility of the mathematical models adjustment (Célino et al. 2014; Hou et al. 2014; Yuan et al. 2019; Consumi et al. 2021). The gathered experimental points plotted as a function of moisture content in cellulose have been shown in **Fig. 4**. Similarly, as in the previous subsection, the dots reflect the recorded data plotted as a function of moisture content. However, this time, adjusting of any regression was not possible. According to the data presented in **Table 2**, none of the investigated models (linear, semilogarithmic, power) did not exhibit a sufficient value of adjusted determination coefficient (R^2 < 90%), hence, indicating inaccurate description of experimental data.

Although the linear regression models were unable to sufficiently reflect the collected experimental points, the data presented in **Fig. 4** contains some important scientific information and deserves a brief discussion.

It might be easily noticed that the behaviour of the maxima differs. Some peaks shift along X axis (peaks no.: 2, 3, 4, 6, 9, 11, 12, 13, 15), while the others remain relatively unchanged (peaks no.: 7, 10, 16) or exhibit specified positions irrespective of the moisture content (peaks no.: 1, 8, 14). Most likely, the shifts described above might be related to the water-cellulose intermolecular interactions and different responses of the specified chemical groups to these attraction forces (Gao et al. 2005; Sun 2008).

The first group distinguished consists of the absorption bands that change the position with increasing moisture content are mostly the signals assigned to polar moieties (able to form hydrogen bonds with water molecules (Luo and Zhu 2010)) and neighbouring to them maxima attributed to non-polar groups

(probably affected by the overlapping of the signals originated from polar moieties (Leszczyńska et al. 2019)). Interestingly, some absorption bands shifted to the lower wavenumbers (peaks no.: 2, 3, 4, 6) while the remaining peaks moved toward higher values of frequency (peaks no.: 9, 11, 12, 13, 15). It is supposed that such a phenomenon is related to the type of interactions created in the water-cellulose system and the reaction of the above-mentioned system to infrared radiation. However, the reason for such a behaviour is not entirely clear and needs to be furtherly analysed in the future.

Moving forward, the maxima that did not significantly change the position along the axis of frequencies are attributed to ring in plane vibrations (peak no. 7) and CH_2 non-polar moieties (peak no. 10) which could be barely affected by water molecules (A.N. and K.J. 2017). However, the last maximum exhibiting relatively stable position is the peak no. 16 assigned to hydroxyl groups that actually might interact with water molecules. On the other hand, based on previously done observations and literature research, it was evidenced that peak no. 16 exhibited relative stability in the position. Firstly, it is partially separated from remaining absorption bands. Therefore, the effect of the signals overlapping is restricted. Secondly, this is the broad maximum consisting of smaller maxima attributed to the inter- and intramolecular hydrogen bonds (Cao and Tan 2004), hence, providing peak's shape stability via dependency on different kinds of interactions.

The last group consists of the absorption bands revealing shifts along the axis of frequencies that are irrespective of the amount of absorbed water. They exhibit a few specified and fixed wavenumber values (especially peaks no.: 8, 14) which does not change describable with increasing moisture content. This means regardless of the amount of absorbed water, these peaks reveal several specific values assigned to the X axis. The behaviour described could be inherent to the material, which is known to be subjected to chemical intrinsic variability (Thygesen et al. 2005; Bourmaud et al. 2018), as well as be assigned to non-specific experimental variations (Garside and Wyeth 2006; Agarwal et al. 2011). However, this phenomenon undoubtedly requires further investigation as its nature is not fully understood.

Summarising, it was not possible to observe the wavenumber-moisture content relationships that could have been described with the investigated regression models. However, data indicating the correlation between the position of the maximum on the axis of frequencies and the moisture content have been gathered. Basing on the collected information, most likely, wavenumber shifts cannot be successfully applied in quantitative assessment of moisture content in cellulose-based materials. Yet, the position of some specific peaks (peaks no.: 2, 3, 4, 6, 9, 11, 12, 13, 15) on the X axis might favourably provide some valuable information on the cellulose-water molecules interactions by applying, e.g., 2Dcos analysis and correlation spectra (Hou et al. 2014), simple calculation of wavenumber shifts (Awa et al. 2014), deconvolutions revealing shifts of hydrogen bonds (Łojewska et al. 2005).

4. Conclusions

For the first time, the variations of both coordinates of sixteen peaks visible in cellulose ATR FT-IR spectrum were successfully investigated and plotted as a function of the moisture content (0.5-11wt.%)

established with Karl-Fischer titration. Regarding the absorbance-water content relationship, data recorded for all considered maxima was fitted with mathematical models exhibiting adjustment of R^2>90% and standard error of prediction approx. 10%. Furthermore, absorption bands that wavenumber shifts could provide significant information on the behaviour of the active centres in cellulose have been favourably defined. Hence, proving ATR FT-IR applicability in quantitative and qualitative analysis of cellulose water content.

Declarations

Ethics approval and consent to participate

All authors approve the submitted version of the manuscript and will to participate.

Consent for publication

All authors agree for publication.

Availability of data and materials

Not applicable

Competing interests

The authors have no relevant financial or non-financial interests to disclose.

Funding

Presented research was realized as a part of the project Diamond Grant financed from the funds of the Ministry of Education and Science in Poland based on contract no. 0238/DIA/2019/48 (project entitled: Hydrophilization of cellulose fibres via hybrid chemical modification).

Authors' contribution

Stefan Cichosz: conceptualization, data analysis, investigation, methodology, formal analysis, writing, **Anna Masek:** conceptualization, data analysis, methodology, review and editing. **Katarzyna Dems-Rudnicka:** development of the statistical methods of data analysis, preparation of the scripts used in the RStudio program. All authors have read and agreed to the published version of the manuscript.

Acknowledgements

This work has been completed while the first author was the Doctoral Candidate in the Interdisciplinary Doctoral School at the Lodz University of Technology, Poland.

References

1. A.N. B, K.J. N (2017) Characterization of alkali treated and untreated new cellulosic fiber from Saharan aloe vera cactus leaves. Carbohydr Polym 174:200–208. https://doi.org/10.1016/j.carbpol.2017.06.065
2. Agarwal V, Huber GW, Conner WC, Auerbach SM (2011) Simulating infrared spectra and hydrogen bonding in cellulose Iβ at elevated temperatures. J Chem Phys 135:. https://doi.org/10.1063/1.3646306
3. Awa K, Shinzawa H, Ozaki Y (2014) An effect of cellulose crystallinity on the moisture absorbability of a pharmaceutical tablet studied by near-infrared spectroscopy. Appl Spectrosc 68:625–632. https://doi.org/10.1366/13-07273
4. Bledzki AK, Faruk O, Huque M (2002) Physico-mechanical studies of wood fiber reinforced composites. Polym - Plast Technol Eng 41:435–451. https://doi.org/10.1081/PPT-120004361
5. Bourmaud A, Beaugrand J, Shah DU, et al (2018) Towards the design of high-performance plant fibre composites. Prog Mater Sci 97:347–408. https://doi.org/10.1016/j.pmatsci.2018.05.005
6. Canteri MHG, Renard CMGC, Le Bourvellec C, Bureau S (2019) ATR-FTIR spectroscopy to determine cell wall composition: Application on a large diversity of fruits and vegetables. Carbohydr Polym 212:186–196. https://doi.org/10.1016/j.carbpol.2019.02.021
7. Cao Y, Tan H (2004) Structural characterization of cellulose with enzymatic treatment. J Mol Struct 705:189–193. https://doi.org/10.1016/j.molstruc.2004.07.010
8. Célino A, Gonçalves O, Jacquemin F, Fréour S (2014) Qualitative and quantitative assessment of water sorption in natural fibres using ATR-FTIR spectroscopy. Carbohydr Polym 101:163–170. https://doi.org/10.1016/j.carbpol.2013.09.023
9. Chen Y, Yu HY, Li Y (2020) Highly Efficient and Superfast Cellulose Dissolution by Green Chloride Salts and Its Dissolution Mechanism. ACS Sustain Chem Eng 8:18446–18454. https://doi.org/10.1021/acssuschemeng.0c05788
10. Cheng K, Heidari Z (2017) Combined interpretation of NMR and TGA measurements to quantify the impact of relative humidity on hydration of clay minerals. Appl Clay Sci 143:362–371. https://doi.org/10.1016/j.clay.2017.04.006
11. Cichosz S, Masek A (2020) IR study on cellulose with the varied moisture contents: Insight into the supramolecular structure. Materials (Basel) 13:. https://doi.org/10.3390/ma13204573
12. Ciolacu D, Ciolacu F, Popa VI (2011) Amorphous cellulose – structure and characterization. Cellul Chem Technol 45:13–21
13. Consumi M, Leone G, Tamasi G, Magnani A (2021) Water content quantification by FTIR in carboxymethyl cellulose food additive. Food Addit Contam - Part A Chem Anal Control Expo Risk Assess 38:1629–1635. https://doi.org/10.1080/19440049.2021.1948619
14. De Caro CA, Aichert A, Walter CM (2001) Efficient, precise and fast water determination by the Karl Fischer titration. Food Control 12:431–436. https://doi.org/10.1016/S0956-7135(01)00020-2
15. Gao ZH, Gu JY, Wang XM, et al (2005) FTIR and XPS study of the reaction of phenyl isocyanate and cellulose with different moisture contents. Pigment Resin Technol 34:282–289.

https://doi.org/10.1108/03699420510620300

16. Garside P, Wyeth P (2006) Identification of cellulosic fibres by FTIR spectroscopy: Differentiation of flax and hemp by polarized ATR FTIR. Stud Conserv 51:205–211. https://doi.org/10.1179/sic.2006.51.3.205
17. Gašparovič L, Koreňová Z, Jelemenský Ľ (2010) Kinetic study of wood chips decomposition by TGA. Chem Pap 64:174–181. https://doi.org/10.2478/s11696-009-0109-4
18. Gulmine J., Janissek P., Heise H., Akcelrud L (2002) Polyethylene characterization by FTIR. Polym Test 21:557–563. https://doi.org/10.1016/S0142-9418(01)00124-6
19. Hofstetter K, Hinterstoisser B, Salmén L (2006) Moisture uptake in native cellulose - The roles of different hydrogen bonds: A dynamic FT-IR study using Deuterium exchange. Cellulose 13:131–145. https://doi.org/10.1007/s10570-006-9055-2
20. Hospodarova V, Singovszka E, Stevulova N (2018) Characterization of Cellulosic Fibers by FTIR Spectroscopy for Their Further Implementation to Building Materials. Am J Anal Chem 09:303–310. https://doi.org/10.4236/ajac.2018.96023
21. Hou L, Feng K, Wu P, Gao H (2014) Investigation of water diffusion process in ethyl cellulose-based films by attenuated total reflectance Fourier transform infrared spectroscopy and two-dimensional correlation analysis. Cellulose 21:4009–4017. https://doi.org/10.1007/s10570-014-0458-1
22. Käppler A, Fischer M, Scholz-Böttcher BM, et al (2018) Comparison of μ-ATR-FTIR spectroscopy and py-GCMS as identification tools for microplastic particles and fibers isolated from river sediments. Anal Bioanal Chem 410:5313–5327. https://doi.org/10.1007/s00216-018-1185-5
23. Kaur R, Singh S, Pandey OP (2012) FTIR structural investigation of gamma irradiated BaO-Na 2O-B 2O 3-SiO 2 glasses. Phys B Condens Matter 407:4765–4769. https://doi.org/10.1016/j.physb.2012.08.031
24. Kondo T, Rytczak P, Bielecki S (2016) Bacterial NanoCellulose Characterization. Elsevier B.V.
25. Lee CM, Kubicki JD, Fan B, et al (2015) Hydrogen-Bonding Network and OH Stretch Vibration of Cellulose: Comparison of Computational Modeling with Polarized IR and SFG Spectra. J Phys Chem B 119:15138–15149. https://doi.org/10.1021/acs.jpcb.5b08015
26. Leszczyńska A, Radzik P, Szefer E, et al (2019) Surface Modification of Cellulose Nanocrystals with Succinic Anhydride. Polymers (Basel) 11:866. https://doi.org/10.3390/polym11050866
27. Łojewska J, Miśkowiec P, Łojewski T, Proniewicz LM (2005) Cellulose oxidative and hydrolytic degradation: In situ FTIR approach. Polym Degrad Stab 88:512–520. https://doi.org/10.1016/j.polymdegradstab.2004.12.012
28. Luo X, Zhu JY (2010) Effects of drying-induced fiber hornification on enzymatic saccharification of lignocelluloses. Enzyme Microb Technol 48:92–99. https://doi.org/10.1016/j.enzmictec.2010.09.014
29. Martin D, Perkasa C, Lelekakis N (2013) Measuring paper water content of transformers: A new approach using cellulose isotherms in nonequilibrium conditions. IEEE Trans Power Deliv 28:1433–1439. https://doi.org/10.1109/TPWRD.2013.2248396

30. Mihranyan A, Llagostera AP, Karmhag R, et al (2004a) Moisture sorption by cellulose powders of varying crystallinity. Int J Pharm 269:433–442. https://doi.org/10.1016/j.ijpharm.2003.09.030
31. Mihranyan A, Pinas Llagostera A, Karmhag R, et al (2004b) Moisture sortpion by cellulose powders of varying crystallinity. Int J Pharm 269:433–442
32. Missoum K, Belgacem MN, Bras J (2013) Nanofibrillated cellulose surface modification: A review. Materials (Basel) 6:1745–1766. https://doi.org/10.3390/ma6051745
33. Morán JI, Alvarez VA, Cyras VP, Vázquez A (2008) Extraction of cellulose and preparation of nanocellulose from sisal fibers. Cellulose 15:149–159. https://doi.org/10.1007/s10570-007-9145-9
34. Oh SY, Dong IY, Shin Y, et al (2005a) Crystalline structure analysis of cellulose treated with sodium hydroxide and carbon dioxide by means of X-ray diffraction and FTIR spectroscopy. Carbohydr Res 340:2376–2391. https://doi.org/10.1016/j.carres.2005.08.007
35. Oh SY, Yoo D Il, Shin Y, Seo G (2005b) FTIR analysis of cellulose treated with sodium hydroxide and carbon dioxide. Carbohydr Res 340:417–428. https://doi.org/10.1016/j.carres.2004.11.027
36. Olsson AM, Salmén L (2004) The association of water to cellulose and hemicellulose in paper examined by FTIR spectroscopy. Carbohydr Res 339:813–818. https://doi.org/10.1016/j.carres.2004.01.005
37. Peršin Z, Stenius P, Stana-Kleinschek K (2011) Estimation of the surface energy of chemically and oxygen plasma-treated regenerated cellulosic fabrics using various calculation models. Text Res J 81:1673–1685. https://doi.org/10.1177/0040517511410110
38. Poletto M, Ornaghi Júnior HL, Zattera AJ (2014) Native cellulose: Structure, characterization and thermal properties. Materials (Basel) 7:6105–6119. https://doi.org/10.3390/ma7096105
39. Przybylek P (2017) Drying transformer cellulose insulation by means of synthetic ester. IEEE Trans Dielectr Electr Insul 24:2643–2648. https://doi.org/10.1109/TDEI.2017.006160
40. R Core Team (2021) R: A language and environment for statistical computing.
41. Salmén L, Bergström E (2009) Cellulose structural arrangement in relation to spectral changes in tensile loading FTIR. Cellulose 16:975–982. https://doi.org/10.1007/s10570-009-9331-z
42. Sun CC (2008) Mechanism of moisture induced variations in true density and compaction properties of microcrystalline cellulose. Int J Pharm 346:93–101. https://doi.org/10.1016/j.ijpharm.2007.06.017
43. Thygesen A, Oddershede J, Lilholt H, et al (2005) On the determination of crystallinity and cellulose content in plant fibres. Cellulose 12:563–576. https://doi.org/10.1007/s10570-005-9001-8
44. Yuan H, Guo X, Xiao T, et al (2019) Moisture adsorption in TEMPO-oxidized cellulose nanocrystal film at the nanogram level based on micro-FTIR spectroscopy. Cellulose 26:7175–7183. https://doi.org/10.1007/s10570-019-02593-9

Figures

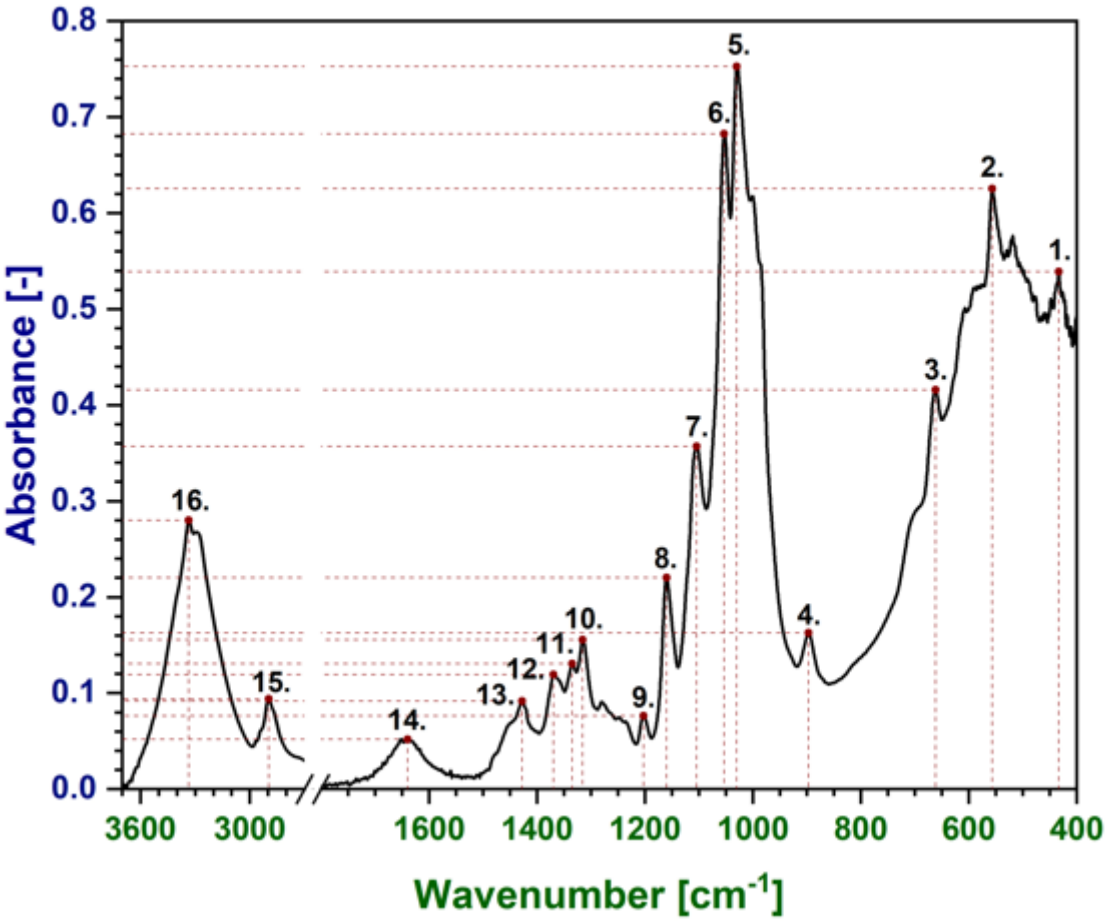

Figure 1

Exemplary ATR FT-IR spectrum of cellulose with the assignment of the peaks analysed. Throughout the whole manuscript absorbance values are marked with dark blue and wavenumber values with dark green.

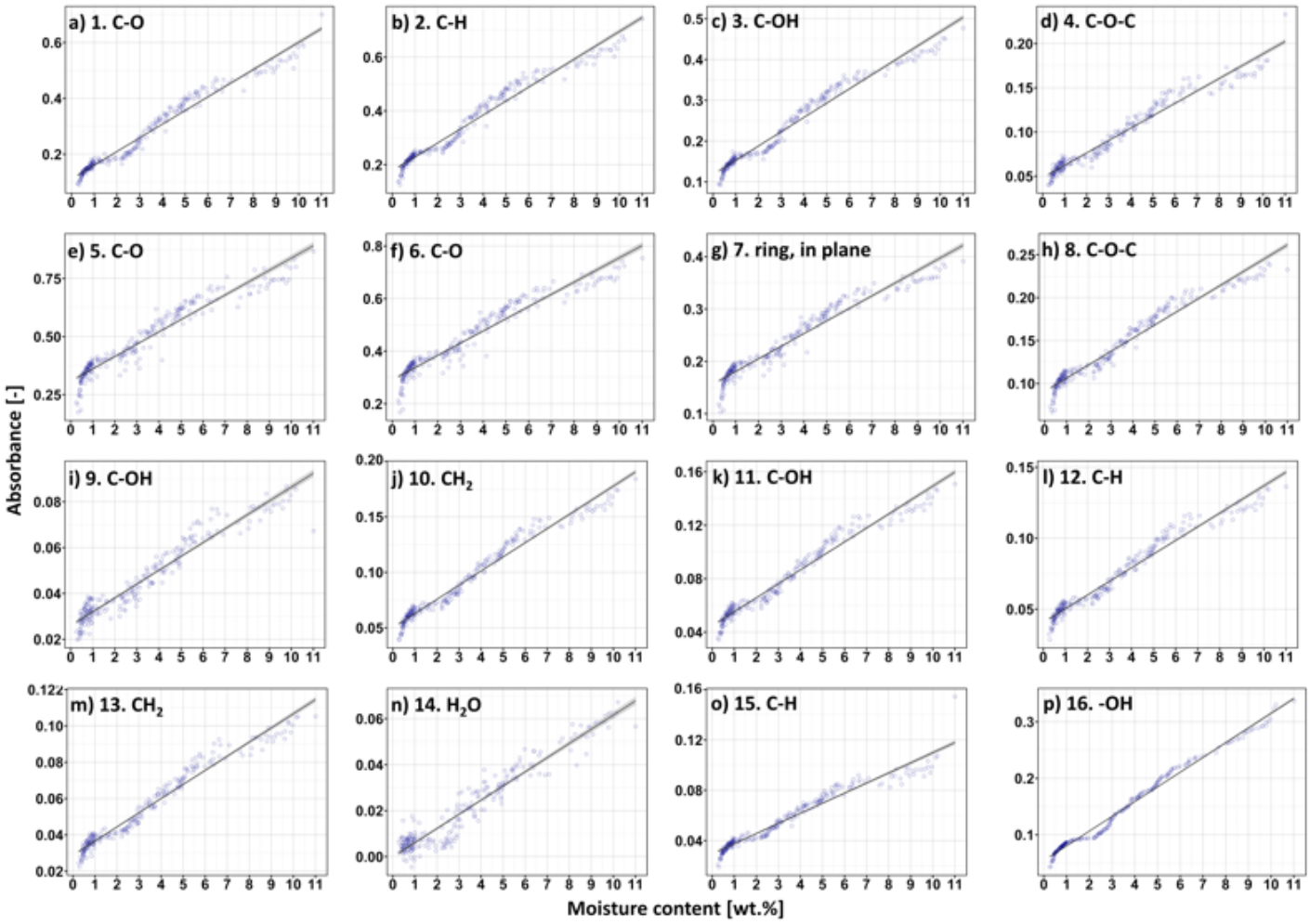

Figure 2

Height of the selected peaks (a-p) plotted as a function of moisture content in cellulose fibres determined through Karl-Fischer titration. Experimentally measured band absorbance (dark blue) and mathematically adjusted regression (black) with marked confidence area (grey).

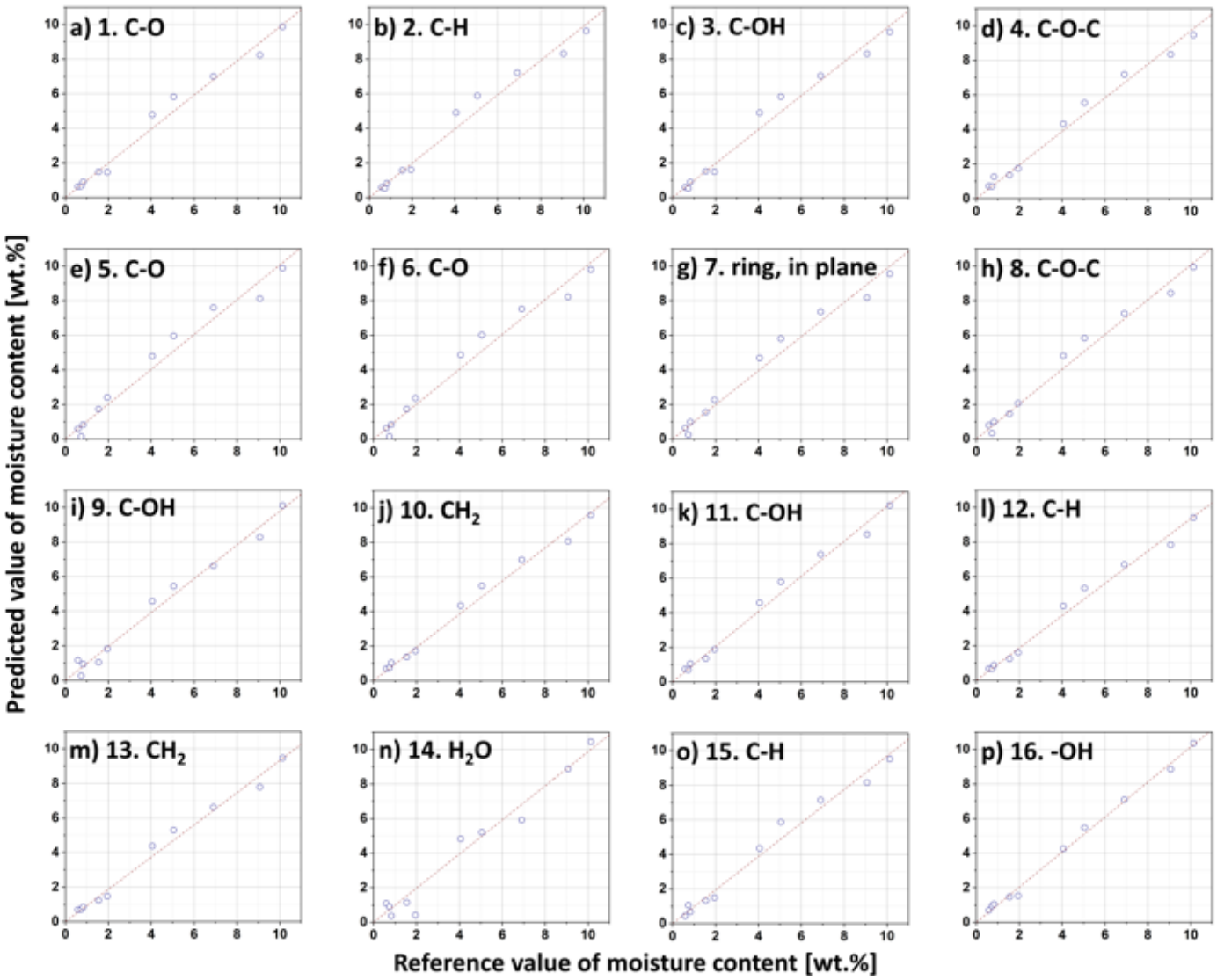

Figure 3

External validation results of water content prediction for cellulose fibres. The predictions of the moisture content obtained with the ATR FT-IR approach were compared to the Karl-Fischer titration measurements.

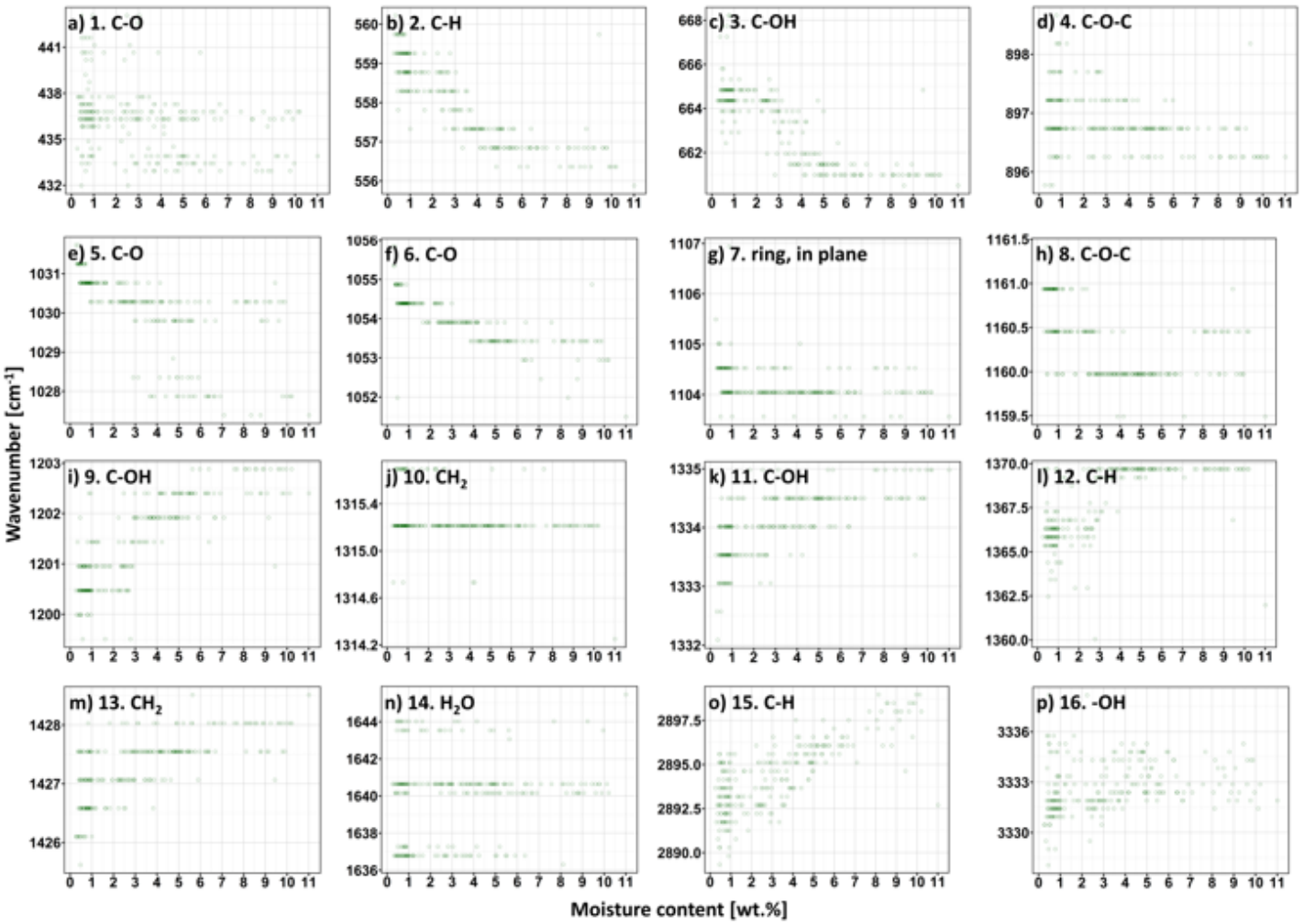

Figure 4

Wavenumber of the selected peaks (a-p) plotted as a function of moisture content in cellulose fibres determined by the means of Karl-Fischer titration. No linear regressions were found.